Online at: https://researchtrendsjournal.com ISSN No: 2584-282X

INTERNATIONAL JOURNAL OF TRENDS IN EMERGING RESEARCH AND DEVELOPMENT

INTERNATIONAL JOURNAL OF TRENDS IN EMERGING RESEARCH AND DEVELOPMENT

Volume 2; Issue 1; 2024; Page No. 100-106

Received: 04-11-2023
Accepted: 19-12-2023

An image fusion and extreme learning adaboost classification algorithm-based effective approach for brain and lung tumor and lung detection and classifications

[1]M Ashwitha and [2]Dr. Manish Saxena

[1]Research Scholar, Department of Computer Science, Himalayan University, Itanagar, Arunachal Pradesh, India
[2]Assistant Professor, Department of Computer Science, Himalayan University, Itanagar, Arunachal Pradesh, India

Corresponding Author: M Ashwitha

Abstract

This paper looks on the abnormalities of the Brain and lung caused by Brain and lung tumors and the lung abnormalities caused by COVID-19. In the course of the lung inquiry, a technique for segmenting the infection from the 3D CT volumes and diagnosing and determining the severity of COVID-19 from 2D CT pictures are proposed. A method of classifying Brain and lung tumors from 2D MRI pictures and segmenting tumors and edema from 3D MRI volumes is proposed for the Brain and lung abnormalities. As a first-line method for detecting severity risks in COVID-19, the proposed approach has a wide range of applications in the medical industry. It can help medical personnel plan patient care and determine whether ICU facilities and ventilator support are necessary. In these uncertain times, a computer-aided system that can assist in creating a treatment plan for the massive influx of patients every day is undoubtedly going to be helpful.

Keywords: Brain, lung caused, MRI volumes

Introduction

The highest mortality rate tumor in the world is known as Brain and lung tumors which leads to death if it is not properly and timely treated. The less aggressive tumors are called as low grade tumors and they are not leads to death in patients. The high aggressive tumors are called as high grade tumors and they lead to death. In present methods, surgery of the affected tumor regions, radiography by sending the high density radio waves through the affected regions and chemotherapy. Some tumor patients require any one of the above mentioned method for treating the tumors. Some patients require the combination of the above methods for effective treatment of the Brain and lung tumors. In point of clinical reference, Magnetic Resonance Imaging (MRI) scanning method is preferred due to the availability of fine information of the Brain and lung regions. The proper treatments planning avoid the earlier death in patients around the world.

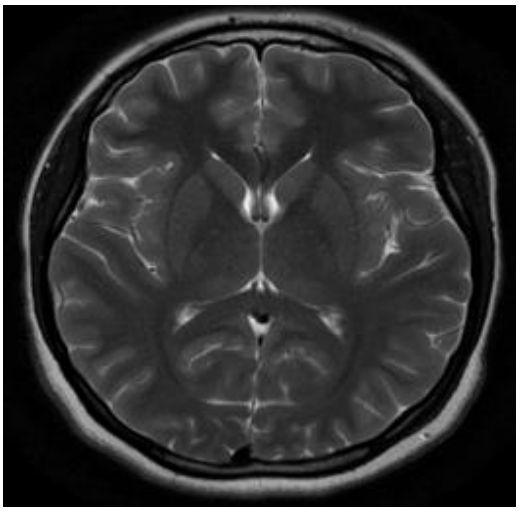

Fig 1: Brain and lung MRI image with no abnormal pixels

The segmentation process plays an important role in tumor treatments planning. In current tumor detection and segmentation methods, linear parametric and non-linear parametric approaches are used to detect and locate the tumor regions in Brain and lung MRI images. Such methods failed to locate the tumor pixels in low contrasted Brain and lung images. Markov Random Fields (MRF) was developed to construct the random metrics of the tumor and non-tumor pixels. This method also suffered by the low tumor segmentation accuracy. Hence, this paper proposes an efficient approach for developing the Brain and lung tumor detection framework using fusion based classification approach.

This work proposes an efficient approach for developing the Brain and lung tumor detection framework using fusion based classification approach. The Brain and lung Magnetic Resonance Imaging (MRI) images from open access dataset are fused with each other to enhance the internal low resolution border pixels. The Curvelet transform is applied now on the fused Brain and lung image for obtaining the non-linear coefficient metric patterns. Then, features are computed from these transformed non-linear coefficient metric patterns and these are further classified by proposed Extreme Learning Adaboost Classification (ELAC) algorithm for differentiating the tumor affected Brain and lung images from non-tumor affected Brain and lung images. This work also uses morphological segmentation algorithm for segmenting the tumor regions in tumor classified Brain and lung MRI images.

Rajan *et al*. (2019) [12] developed Brain and lung tumor detection system using intensity adjustment algorithm. The k-means clustering algorithm was integrated with fuzzy –c means classification algorithm and this hybrid algorithm was applied on the source Brain and lung MRI image for detecting and locating the abnormal tumor pixels in an image. The active contour model was developed for segmenting the tumor pixels in edge regions. The authors obtained 96.6% of sensitivity and 97.1% of tumor pixel segmentation accuracy. Sajid *et al*. (2019) [12] applied deep learning algorithm on Brain and lung MRI images for the classification and detection of abnormal Brain and lung tumors. This patch based approach extracted contextual information from each pixel in source image and they were trained and classified using deep neural networks. The authors obtained 86% of sensitivity and 91% of specificity as performance estimation parameters. Rajagopal (2019) [12] applied random forest classification algorithm with its improved weighted technique on Brain and lung images to detect and locate the tumor regions. The ant colony features were derived from the source Brain and lung image and these computed features were optimized using Genetic Algorithm (GA) based optimization technique. The optimized features were classified using weighted random forest classification approach and this method obtained the sensitivity rate of 97.7%, specificity rate of 96.5% and the tumor segmentation accuracy rate of 98.01% on BRATS 2015 dataset.

El-Melegy *et al*. (2014) [11] detected and segmented the abnormal tumor pixels in the Brain and lung MRI image using fuzzy based approach. The authors constructed linear contour modeling framework for extracting the contour points in border pixels. The features were computed from each border pixel points and they were classified using fuzzy rule based classification algorithm. This proposed method classified the Brain and lung MRI images which were available in open access dataset and obtained 95.1% of classification rate.

Materials and Methods

Materials

This paper uses two different publicly available Brain and lung image datasets BRATS 2015 and Brain and lung Web. From BRATS 2015 dataset, 129 normal Brain and lung MRI images and 78 abnormal Brain and lung images are obtained. From Brain and lung Web dataset, 162 normal Brain and lung MRI images and 65 abnormal Brain and lung MRI images are obtained. Both Brain and lung image datasets are having its own ground truth images. The Brain and lung Web dataset images are classified into T1-, T2-, and Proton Density (PD) weighted images. The images in BRATS dataset are having the specifications of 512*512 pixels as width and height and the images in Brain and lung Web dataset are having the specifications of 256*256 pixels as width and height.

Methods

This work proposes an efficient approach for developing the Brain and lung tumor detection framework using fusion based classification approach. The Brain and lung MRI images from open access dataset are fused with each other to enhance the internal low resolution border pixels. The Curvelet transform is applied now on the fused Brain and lung image for obtaining the non-linear coefficient metric patterns. Then, features are computed from these transformed non-linear coefficient metric patterns and these are further classified by proposed Extreme Learning Adaboost Classification (ELAC) algorithm for differentiating the tumor affected Brain and lung images from non-tumor affected Brain and lung images.

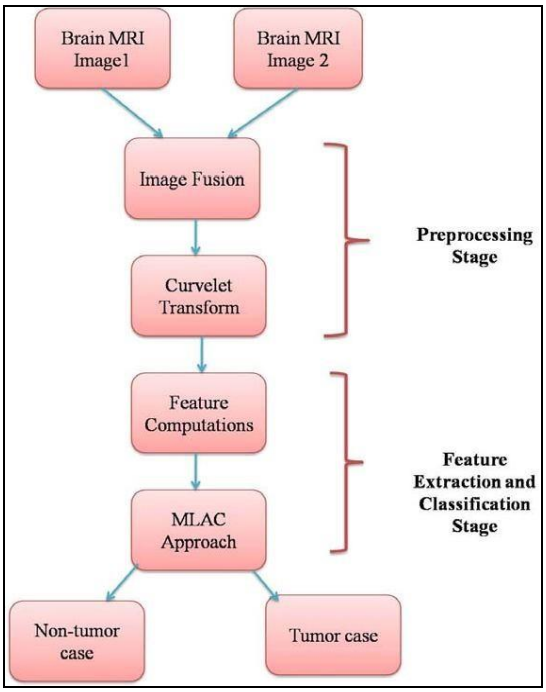

Fig 2: Detailed developments of proposed brain and lung Tumor detection and classification system

Image Fusion

This work proposes an efficient approach for developing the Brain and lung tumor detection framework using fusion based classification approach. The Brain and lung MRI images from open access dataset are fused with each other to enhance the internal low resolution border pixels. The Curvelet transform is applied now on the fused Brain and lung image for obtaining the non-linear coefficient metric patterns. Then, features are computed from these transformed non-linear coefficient metric patterns and these are further classified by proposed Extreme Learning Adaboost Classification (ELAC) algorithm for differentiating the tumor affected Brain and lung images from non-tumor affected Brain and lung images.

Figure 2 shows the detailed developments of proposed Brain and lung tumor detection and classification system.

$A(N, n) = \sum \sum Hr{-}2N * Hc{-}2n * Cj$ (1.1)

$H(N, n) = \sum \sum Gr{-}2N * Hc{-}2n * Cj$ (1.2)

$V(N, n) = \sum \sum Hr{-}2N * Gc{-}2n * Cj$ (1.3)

$D(N, n) = \sum \sum Gr{-}2N * Gc{-}2n * Cj$ (1.4)

The second stage of image enhancement is applying the fusion rules on the decomposed sub band images as stated as,

$F = HrHc * Cy + HrGc * Cy + GrHc * Cy + GrGc * Cy$ (1.5)

The fused Brain and lung image is depicted in Figure 3.

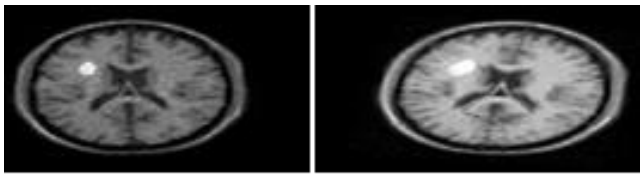

Fig 3(a): Brain and lung MRI image and (b) enhanced image using image fusion

Curvelet Transform

The multi layer and level decomposition of an image can be done by Curvelet transform. The reconstruction rate is high when compared with other conventional transforms and also its directionality behavior is high in Curvelet domain. The scaling parameter of Curvelet transform is parabolic type and it is represented as 2-j. It can be operated with respect to various angles of orientations and scales. In general, Curvelet transform can be derived from Fourier transform as stated below.

$(w) = FT(w)$ (1.6)

Where, i(w) is the coefficient if Curvelet transform at scale 2-j with the orientation of the Cartesian function can be used to define the Curvelet transform as stated in the following equation.

$(w) = iR8(I - Ii))$ (1.7)

Where, R8 is the angle of orientation, I (i,j) is the source Brain and lung MRI image in time domain and Ii is the image with its scaling domain.

The Curvelet transform can be expressed with its scaling function by the following equation.

$C(i, j) = f\ I(i, j) * \square i(w) * dw$ (1.8)

Figure-4 shows the Curvelet transform implications in multi scale and multi orientation domain format.

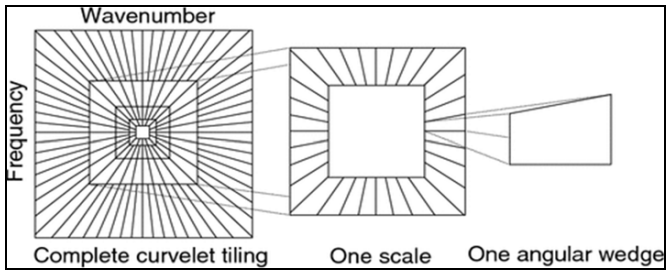

Fig 4: Curvelet Transform Implications

Feature Computations - GLCM

This paper computes Grey Level Co-occurrence Matrix (GLCM) features from the transformed non-linear coefficients of Curvelet transform at the angle of orientation 45 degree. The following features are computed from these transformed coefficients for identifying or classifying the tumor images from non-tumor images. Let C(i, j) be the coefficient value of Curvelet transform in the form of matrix by its size M, with its rows and columns are represented as 'i' and 'j'.

The feature 'Contrast' is extracted from the non-linear matrix for differentiating the bright pixel from the dark pixels in a Brain and lung MRI image. Dissimilarity metric feature is used to highlight the dissimilar variability between each pixel in a Brain and lung image. These features are explained in the following equations.

$\text{Contrast} = \sum^{M-1} C(i, j)^2$ (1.9)

$\text{DISSINILARITY} = \sum^{M-1} |i - j| * C(i, j)$ (1.10)

The compactness of the each pixel along with its surrounding pixels in an image is measured using its homogeneity value.

$$\text{HONOGENEITY} = \sum_{i,j=0}^{M-1} \frac{C(i,j)}{1+|i-j|^2} \quad (1.11)$$

The non-linear relationship between every pixel along with its surrounding pixels is defined by Energy and Correlation.

$$\text{Energy} = \sum_{i,j=0}^{M-1} C(i, j)^2 \quad (1.12)$$

$$\text{Correlation} = \sum_{i,j=0}^{M-1} C(i, j) * \frac{(i-\mu)*(j-\mu)}{o^2} \quad (1.13)$$

where, μ and o are the mean and standard deviation of the extracted non-linear coefficient matrix.

ELAC approach

The classification algorithms are used to differentiate the tumor affected image from normal Brain and lung images using the extracted feature set. Many researchers used Support Vector Machine (SVM) and Adaptive Neuro Fuzzy Inference System (ANFIS) classification approaches for detecting the tumor affected images. The classification rate of these conventional classification algorithms is not optimum and hence this paper uses ELAC algorithm for the classification of tumor affected Brain and lung images from

normal Brain and lung images.
This algorithm is explained in the following steps.

ELAC algorithm
Inputs: Extracted feature sets;
Output: classification results; Start;

Step 1: Compute the weight density distribution function of each extracted feature samples using the following equation.

$$W_i = \frac{1}{1+e^{-x_j\mu}} \quad (1.14)$$

Step 2: Find the error rate of each extracted feature samples with its weight density function as stated below.

$$e_i = \frac{1}{2} * \ln \frac{1-Mi}{M_i} \quad (1.15)$$

Step 3: Determine the ensemble fractional rate index of each extracted feature samples as,

$$EFRi = Wi * Fi + \sum N \quad ei * Fi \quad (1.16)$$

Step 4: Find the classification index using weight density distribution function, error rate and ensemble fractional rate index, using the following equation stated as,

$$CI = \frac{EFR_j * \exp(Ki * e_j)}{M_i} \quad (1.17)$$

Step 5: The tumor Brain and lung images can be determined using the following constraint.

$$\text{INAGEClassifications} = \{ \begin{matrix} \text{TUNOR; ifCI} \geq 0 \\ \text{Non} - \text{TUNOR; else} \end{matrix} \} \quad (1.18)$$

Segmentation
This study employs morphological segmentation technique for segmenting the tumor areas in tumor categorized Brain and lung MRI images, as displayed in Figure-5. The dialtion procedure uses the structuring element of 2 radius as indicated in the following equation to fill in the gaps in each pixel of the Brain and lung picture impacted by an identified abnormal tumor.

D = iNfill (I, *h*oles, se = 2) (1.19)

The erosion process removes the holes in each pixel of the classified abnormal tumor affected Brain and lung image using the structuring element of 1 radius as stated in the folloiwng equation.

E = INERODE (I, erode, se = 1) (1.20)

Then, morphological subtraction function is applied between D and E for segmenting the tumor region in Brain and lung MRI image, as indicated in the folloiwng equation.
TUNORREGION = iNSUBTRACT (D, E) (1.21)

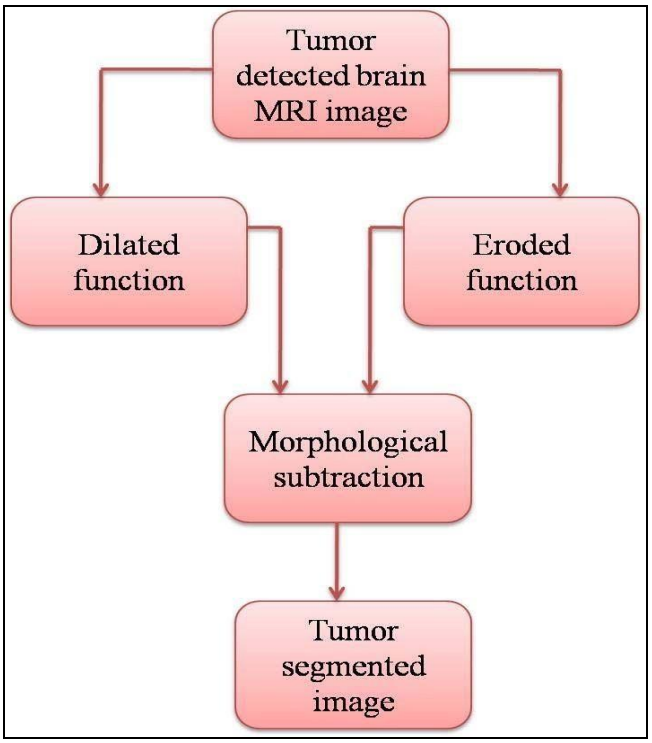

Fig 5: Morphological Segmentation Process Flow

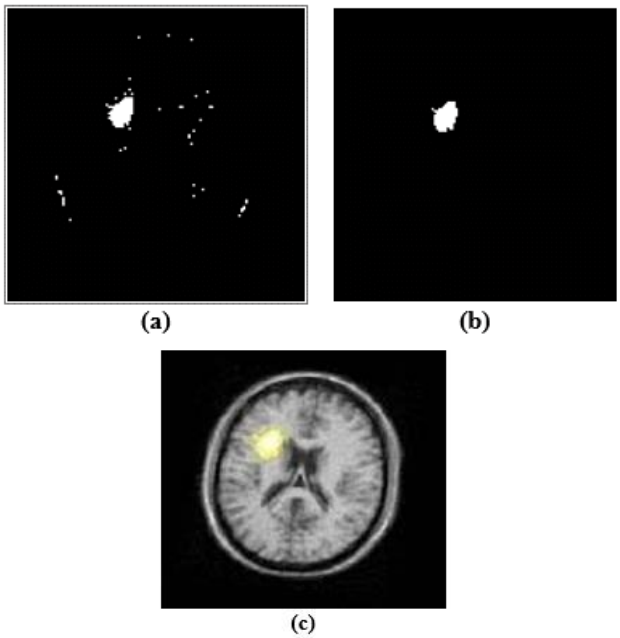

Fig 6: (A) Dilated Image (B) Eroded Image And (C) Tumour Region Marked Brain and Lung Mri Image

Results And Discussions
From the segmented tumor regions in Brain and lung MRI image, the morphological parameters are extracted from these tumor segmented regions. The computed morphological parameters from segmented tumor regions are Area, Perimeter, Circularity, Eccentricity, Minimum Intensity, Maximum Intensity and Diameter. Standard clinical reference values are assigned to these morphological parameters.
Morphological study of segmented tumor areas in relation to pictures from the Brain and lung Web dataset and the

BRATS 2015 dataset is shown in Table-1. The clinical reference values of each morphological parameter are supplied with its maximum and minimum reference limit.

Table 1: Morphological analysis of segmented tumor regions with respect to different datasets

Morphological parameters	Clinical reference value	
	BRATS 2015 dataset	Brain and lung web dataset
Area	217±14	198± 12
Perimeter	64.3± 1.3	56.8±1.5
Circularity	0.721±0.4	0.67±0.47
Eccentricity	0.873±0.3	0.769±0.23
Minimum Intensity	72±12	67± 5
Maximum Intensity	257	250±7
Diameter	127± 2.5	122± 1.4

The morphological analysis of segmented tumor regions using the BRATS 2015 dataset in relation to the suggested ELAC classification approach is presented in Table-2.

Table 2: Morphological analysis of segmented tumor regions with respect to the proposed elect classification approach on brats 2015 dataset

Morphological parameters	Proposed ELAC Approach
Area	217
Perimeter	64.3
Circularity	0.723
Eccentricity	0.854
Minimum Intensity	67
Maximum Intensity	258
Diameter	123

Table-3 shows the morphological analysis of segmented tumor regions with respect to different classification approaches on BRATS 2015 dataset. From Table-3, it is quite obvious that the proposed ELAC technique identifies and segments the tumor locations in Brain and lung MRI images when compared with traditional ANFIS classification strategy on the Brain and lung MRI images available in BRATS 2015 dataset.

Table 3: Morphological analysis of segmented tumor regions with respect to different classification approaches on brats 2015 dataset

Morphological parameters	Classification Methods	
	Proposed ELAC Approach	Conventional ANFIS classification Approach
Area	217	193
Perimeter	64.3	60.4
Circularity	0.722	0.565
Eccentricity	0.854	0.654
Minimum Intensity	67	47
Maximum Intensity	258	203
Diameter	123	105

The graphical plot of the morphological analysis of segmented tumor regions on the BRATS 2015 dataset is displayed in Figure 7.

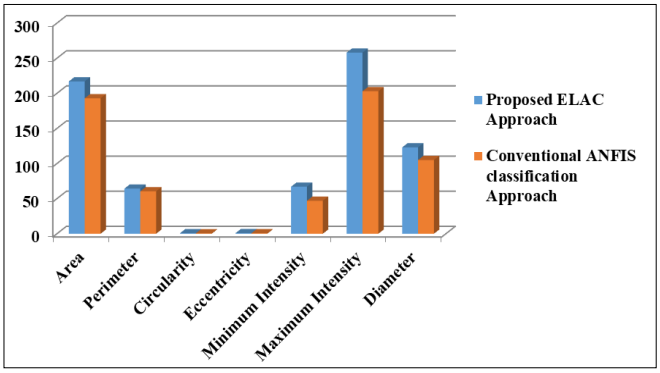

Fig 7: Graphical plot of morphological analysis of segmented tumor regions on brats 2015 dataset

The morphological examination of segmented tumor areas using the Brain and lung Web dataset in accordance with the suggested ELAC classification technique is presented in Table-4.

Table 4: Morphological analysis of segmented tumor regions with respect to the proposed elac classification approach on brain and lungweb dataset

Morphological parameters	Proposed ELAC Approach
Area	193
Perimeter	55.5
Circularity	0.63
Eccentricity	0.757
Minimum Intensity	67
Maximum Intensity	255
Diameter	120.3

Table 5 shows the morphological analysis of segmented tumor regions with respect to different classification approaches on Brain and lung Web dataset. When compared to the traditional ANFIS classification technique on the Brain and lung MRI pictures provided in the Brain and lung Web dataset, Table-5 makes it abundantly evident that the suggested ELAC approach finds and segments the tumor locations in Brain and lung MRI images.

Table 5: Morphological analysis of segmented tumor regions with respect to different classification approaches on brain and lungweb dataset

Morphological parameters	Classification Methods	
	ELAC Approach	ANFIS classification Approach
Area	193	187
Perimeter	55.5	45.7
Circularity	0.63	0.55
Eccentricity	0.758	0.385
Minimum Intensity	67	43
Maximum Intensity	255	194
Diameter	120.3	115.4

The graphical plot of the Brain and lungWeb dataset's segmented tumor regions' morphological analysis is displayed in Figure-8.

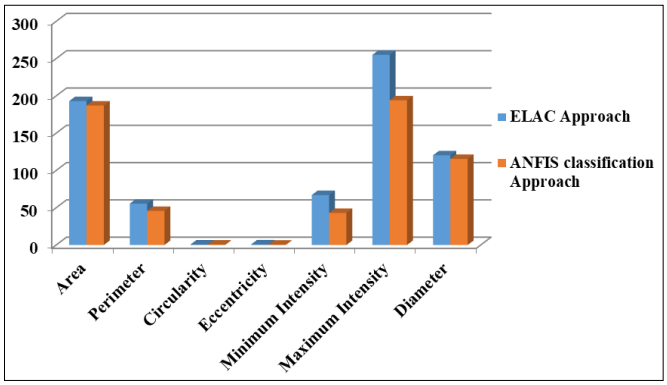

Fig 8: Graphical plot of morphological analysis of segmented tumor regions on brain and lungweb Dataset

To assess the performance analysis of the suggested ELAC approach, the following index metric parameters are also applied with segmented tumor regions.

$$\text{Sensitivity(Se)} = \frac{TP * 100\%}{TP+FN} \quad (1.22)$$

$$\text{Specificity (Sp)} = \frac{TN * 100\%}{TN+FP} \quad (1.23)$$

$$\text{Accuracy (Acc)} = \frac{TP+TN * 100\%}{TP+TN+FP+FN} \quad (1.24)$$

Table-6 presents the analysis of Index metric parameters of tumor regions that have been segmented according to various classification approaches using the BRATS 2015 dataset. The suggested ELAC technique yields 98.5% of sensitivity, 98.7% of specificity and 99.5% of accuracy on BRATS 2015 dataset. The ANFIS classification approach is also applied on the same picture sequences in BRATS 2015 dataset and it obtained 96.7% of sensitivity, 97.4% of specificity and 97.8% of accuracy.

Table 6: Index metric parameters analysis of segmented tumor regions with respect to different classification approaches on brats 2015 dataset

Image sequences	Proposed ELAC Approach			Image registration based ANFIS approach			Sasikanth *et al.* (2018)		
	Se (%)	Sp (%)	Acc (%)	Se (%)	Sp (%)	Acc (%)	Se (%)	Sp (%)	Acc (%)
Image1	98.3	98.5	99.3	95.4	97.4	98.5	96.3	97.3	97.3
Image2	98.3	98.7	99.3	96.3	98.3	98.7	96.4	97.4	97.7
Image3	98.7	98.5	99.7	97.3	98.5	99.3	97.3	97.3	97.7
Image4	98.8	98.5	99.7	94.4	96.7	99.7	95.7	97.3	97.5
Image5	98.4	98.7	99.5	93.7	98.7	97.7	98.7	97.7	97.8
Image6	98.7	98.7	99.7	98.5	98.5	98.3	96.3	97.4	98.3
Image7	98.3	98.4	99.4	96.4	96.4	98.5	96.4	97.3	97.6
Image8	98.7	98.7	99.5	95.8	94.7	98.3	97.3	97.7	97.3
Image9	98.5	98.3	99.7	96.3	98.3	99.8	96.4	97.3	98.3
Image10	98.3	98.4	99.3	97.7	98.5	98.5	96.5	97.3	98.5
Average	98.3	98.5	99.7	96.4	97.5	98.5	96.5	97.8	97.4

The graphical depiction of the segmented tumor areas' analysis using the Index metric parameters on the BRATS 2015 dataset is displayed in Figure 9.

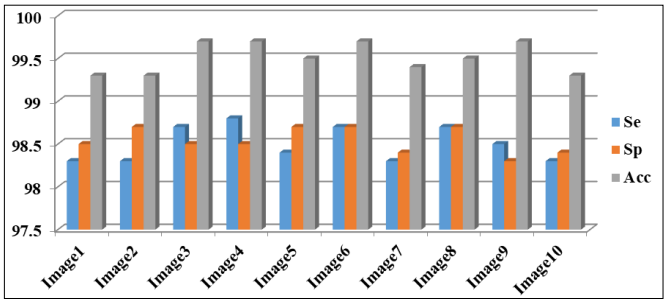

Fig 9: Graphical plot of index metric parameters analysis of segmented tumor regions on brats 2015 dataset

The segmented tumor areas' Index metric parameters analysis for various classification strategies using the Brain and lung Web dataset is displayed in Table-7. On the BRATS 2015 dataset, the suggested ELAC method achieves 97.3% sensitivity, 98.4% specificity, and 99.3% accuracy. The ANFIS classification algorithm is also applied on the same picture sequences in BRATS 2015 dataset and it obtained 96.7% of sensitivity, 97.7% of specificity and 98.3% of accuracy.

Table 7: Index metric parameters analysis of segmented tumor regions with respect to different classification approaches on brain and lungweb dataset

Image sequences	Proposed ELAC Approach			Image registration based ANFIS approach			Sasikanth *et al.* (2018)		
	Se (%)	Sp (%)	Acc (%)	Se (%)	Sp (%)	Acc (%)	Se (%)	Sp (%)	Acc (%)
Image1	98.4	99.4	99.5	99.3	98.5	99.5	96.4	97.3	97.7
Image2	98.7	98.3	99.8	98.4	98.7	98.3	96.3	97.3	98.3
Image3	98.3	98.7	99.4	99.5	98.7	97.7	96.7	97.7	98.4
Image4	98.7	99.8	98.3	98.3	99.3	98.3	97.3	97.7	97.7
Image5	98.3	99.3	98.7	97.7	99.5	98.7	97.7	97.4	97.4
Image6	98.7	98.7	99.3	98.9	98.3	98.3	96.3	97.5	97.7
Image7	98.7	99.5	99.3	98.4	98.4	99.8	96.7	97.	98.7
Image8	98.3	98.7	99.7	98.7	98.7	98.5	98.5	98.1	98.4
Image9	98.5	99.3	98.3	97.4	99.7	98.8	96.4	97.3	97.5
Image10	98.4	99.7	98.5	96.5	97.5	98.5	96.7	97.7	98.3
Average	98.54	99.14	99.18	98.8	98.4	98.5	96.7	97.7	98.3

The Index metric parameters on pictures from the BRATS 2015 dataset are compared to the suggested ELAC methodology and the traditional ANFIS classification methods in Table-8.

Table 8: Comparisons of index metric parameters on brats 2015 dataset

Index metric parameters (%)	BRATS 2015 dataset		
	Proposed ELAC Approach	Image registration based ANFIS approach	Sasikanth *et al.* (2018)
Sensitivity	98.54	98.8	96.5
Specificity	99.14	98.4	97.8
Accuracy	99.18	98.5	97.4

The graphical depiction of the segmented tumor areas' analysis using the Brain and lung Web dataset's Index metric parameters is displayed in Figure-9. Figure Graphical plot of index metric parameters analysis of segmented tumor regions on Brain and lung Web dataset

The Index metric parameters on pictures from the Brain and lung Web dataset are compared in Table-9 between the suggested ELAC methodology and the traditional ANFIS classification methods.

Table 9: Comparisons of index metric parameters on brain and lungweb dataset

Index metric parameters (%)	Brain and lung Web dataset		
	Proposed ELAC Approach	Image registration based ANFIS approach	Sasikanth *et al.* (2018)
Sensitivity	98.54	98.8	96.7
Specificity	99.14	98.4	97.7
Accuracy	99.18	98.5	98.3

Conclusion

The internal low resolution border pixels are improved by fusing the Brain and lung MRI images from the public dataset. In order to acquire the non-linear coefficient metric patterns, the merged Brain and lung picture is now subjected to the Curvelet transform. In order to distinguish Brain and lung pictures impacted by tumors from Brain and lung images unaffected by tumors, features are then generated from these altered non-linear coefficient metric patterns and subsequently categorized using the suggested Extreme Learning Adaboost Classification (ELAC) method. On the BRATS 2015 dataset, the suggested ELAC technique achieves 98.5% sensitivity, 98.7% specificity, and 99.5% accuracy. On the BRATS 2015 dataset, the suggested ELAC method achieves 97.6% sensitivity, 98.2% specificity, and 99.1% accuracy.

References

1. Abd-Ellah MK, Awad AI, Khalaf AA, Hamed HF. Design and implementation of a computer-aided diagnosis system for brain tumor classification. In: 28th International Conference on Microelectronics (ICM); c2016. p. 73-76.
2. Barstugan M, Ozkaya U, Ozturk S. Coronavirus (covid-19) classification using ct images by machine learning methods. arXiv preprint. 2020 Mar 20. arXiv:2003.09424.
3. Bartlett P, Freund Y, Lee WS, Schapire RE. Boosting the margin: A new explanation for the effectiveness of voting methods. The annals of statistics. 1998;26(5):1651-86.
4. Castellino RA. Computer aided detection (CAD): an overview. Cancer Imaging. 2005;5(1):17.
5. Erihov M, Alpert S, Kisilev P, Hashoul S. A cross saliency approach to asymmetry-based tumor detection. In: International Conference on Medical Image Computing and Computer-Assisted Intervention. Springer; c2015. p. 636-643.
6. Ghassemi N, Shoeibi A, Rouhani M. Deep neural network with generative adversarial networks pre-training for brain tumor classification based on MR images. Biomedical Signal Processing and Control. 2020;57:101678.
7. Harmon SA, Sanford TH, Xu S, Turkbey EB, Roth H, Xu Z, *et al*. Artificial intelligence for the detection of COVID-19 pneumonia on chest CT using multinational datasets. Nature communications. 2020;11(1):1-7.
8. Jin C, Chen W, Cao Y, Xu Z, Tan Z, Zhang X, *et al*. Development and evaluation of an AI system for COVID-19.
9. Krizhevsky A, Sutskever I, Hinton GE. Imagenet classification with deep convolutional neural networks. Advances in neural information processing systems. 2012;25.
10. Manapure P, Likhar K, Kosare H. Detecting COVID-19 in X-ray images with keras, tensor flow, and deep learning. assessment. 2020 Sep 5;2(3).
11. Nandpuru HB, Salankar SS, Bora VR. MRI brain cancer classification using support vector machine. In: 2014 IEEE Students' Conference on Electrical, Electronics and Computer Science. 2014. p. 1-6.
12. Nasrullah N, Sang J, Alam MS, Mateen M, Cai B, Hu H. Automated lung nodule detection and classification using deep learning combined with multiple strategies. Sensors. 2019 Sep;19(17):3722.
13. Pathak Y, Shukla PK, Tiwari A, Stalin S, Singh S. Deep transfer learning based classification model for COVID-19 disease. Irbm. 2020 Oct 1.
14. Schapire RE. Explaining adaboost. In: Empirical inference. Springer, Berlin, Heidelberg; 2013. p. 37-52.
15. Wang L, Lin ZQ, Wong A. Covid-net: A tailored deep convolutional neural network design for detection of covid-19 cases from chest x-ray images. Scientific Reports. 2020;10(1):1-12.
16. Yan Q, Wang B, Gong D, Luo C, Zhao W, Shen J, *et al*. COVID-19 chest CT image segmentation–A deep convolutional neural network solution. arXiv preprint. 2020 Apr 23. arXiv:2004.10987.
17. Zheng C, Deng X, Fu Q, Zhou Q, Feng J, Ma H, *et al*. Deep learning-based detection for COVID-19 from chest CT using weak label. MedRxiv. 2020 Apr 17.